

Effects of Fe₂O₃ addition and mechanical activation on thermochemical heat storage properties of the Co₃O₄/CoO system

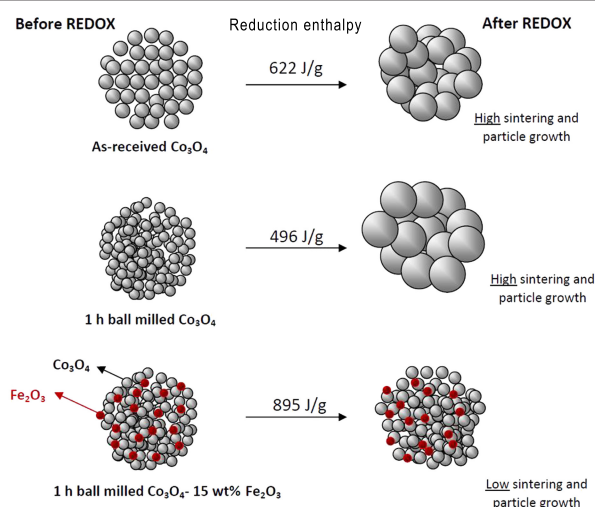
Nariman Nekokar, Mehdi Pourabdoli*, Ahmad Ghaderi Hamidi

Advanced & Energy Storage Materials Lab., Department of Metallurgy and Materials Engineering, Hamadan University of Technology, Hamadan, Iran

HIGHLIGHTS

- Effects of Fe₂O₃ addition and 1 h ball milling on redox reactions of Co₃O₄ were studied.
- Some of the Fe₂O₃ reduced to Fe₃O₄ during the reduction process.
- ΔH_{Red} of Co₃O₄, 1 h ball milled Co₃O₄, and 1 h ball milled Co₃O₄-15 wt% Fe₂O₃ are 622, 496, and 895 kJ/kg, respectively.
- Fe₂O₃ addition and ball milling improved the redox cyclability of Co₃O₄.

GRAPHICAL ABSTRACT



ARTICLE INFO

Article history:

Received 31 December 2017

Revised 1 June 2018

Accepted 10 June 2018

Keywords:

Thermochemical
Heat storage
Cobalt oxide
Sintering
Redox cyclability

ABSTRACT

Effects of Fe₂O₃ addition (2–20 wt%) with 1 h mechanical activation on redox reactions of Co₃O₄ were studied by TG/DSC, SEM, and XRD analyses. The results showed that a Fe₂O₃ addition from 2 to 15 wt% increases the oxygen release from 1.4 to 3.4 wt% and decreases the reduction onset temperature from 1030 to 960 °C, while it increases the oxygen uptake value and re-oxidation onset temperature respectively from 1.5 to 3.3 wt% and from 930 to 1010 °C. The increase in iron oxide to 20 wt% resulted in loss of heat storage properties due to significant reduction in oxygen release and uptake. Moreover, TG/DSC analyses revealed that reduction enthalpy of as-received Co₃O₄, 1 h ball milled Co₃O₄, and 1 h ball milled Co₃O₄-15% Fe₂O₃ are 622, 496, and 895 kJ/kg, respectively. Phase identification and TG experiments under argon atmosphere demonstrated that Fe₂O₃ participates in the reduction process. Furthermore, adding 15 wt% of iron oxide to cobalt oxide and 1 h mechanical activation improved the redox cyclability of cobalt oxide.

* Corresponding author: Tel.: +9881-38411465 ; Fax: +9881-38380520 ; E-mail address: mpourabdoli@hut.ac.ir

DOI: 10.22104/jpsst.2018.2799.1116

1. Introduction

Fossil fuels supply most of the required energy consumption in the world. However, the increasing growth in energy consumption, environmental concerns due to greenhouse emissions and global warming, and depletion of fossil fuels reserves have caused the world to make a serious decision to obtain energy using renewable sources [1,2]. Therefore, it is very important to develop new environmental friendly technologies working with renewable energies. Using concentrated solar power (CSP) along with thermal energy storage (TES) to produce electricity is one of these technologies [3-7]. The main advantage of Solar Thermal Power Plants working with CSP rather than other solar energy technologies is that the heat originated from solar energy can be stored and converted to electricity in off-shine hours thus making dispatch-ability for solar power plants [2]. Among the various CSP technologies, solar towers offer the potential of high temperatures and thus high thermodynamic conversion efficiencies [8,9].

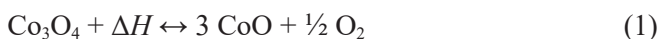
Three methods including sensible, latent, and thermochemical heat storage are used for thermal energy storage [10,11]. The concept of thermochemical heat storage was first introduced by Funk and Reinstorm in 1966 [12]. In fact, the thermochemical heat storage method is based on redox reactions and exploits the heat effects of reversible chemical reactions [10]. Thermochemical heat storage has the advantages of higher energy storage, suitability for large-scale applications, long storage duration and long-range transport at ambient temperature, and higher working temperature ranges in comparison with the other two storage methods [11,13].

Various reversible reactions have been studied for thermochemical heat storage. They include carbonation/decarbonation of metal oxides/carbonates [14,15], hydration/dehydration of metal hydroxides [16-18], decomposition/sulfation of metal sulfates/oxides [1,19], ammonia synthesis/dissociation [20] and reduction/oxidation (redox) of metal oxides [14]. Among these, metal oxides have the main advantage of incorporation with air-operated solar thermal power plants. Attractive mono-metallic redox pair oxides are those which are capable of taking up and releasing gas-phase O₂ at conditions relevant for generation of heat [14,21,22] including Co₃O₄/CoO [22-25], BaO₂/BaO [26], Mn₂O₃/Mn₃O₄ [2,27,28], CuO/Cu₂O [29], Fe₂O₃/Fe₃O₄ [30].

Multi-metallic redox oxides such as perovskites [31-33] have been recently investigated.

According to Wong *et al.* [34] only a few metal oxides have the required properties for thermochemical heat storage including Co₃O₄, BaO₂, Mn₂O₃, CuO, Fe₂O₃, Mn₃O₄ and V₂O₅, with an emphasis that cobalt oxide shows the best re-oxidation kinetics.

Cobalt oxide is one of the most promising materials for thermochemical heat storage. The redox temperature for the Co₃O₄/CoO pair is about 885-905 °C according to Eq. (1) [35]:



$$\Delta H = 200 \text{ kJ/mol}_{\text{react}} \text{ or } 844 \text{ kJ/kg}_{\text{react}}$$

Cobalt oxide has been studied using various reactors such as directly irradiated rotary kiln and powder-coated honeycomb reactors [24,36]. The reduction and re-oxidation of cobalt oxide powder for 30 cycles in a solar-heated rotary kiln were studied by Neises *et al.* [24]. They achieved a storage capacity of about 400 kJ/kg in a cycle with half reduced material due to insufficient mixing. Agrafiotis *et al.* [8,23,35] studied the porous foams and pellets made of Co₃O₄ for about 30 redox cycles. They found that foam retained its integrity and stoichiometric redox performance after the cycles, while pellets exhibited cracks after a few cycles. They also stated that when using foams or pellets of Co₃O₄, all the oxide is exploited for the thermochemical reaction. According to research by Karagiannakis *et al.* [37], a gravimetric energy storage density of 495 kJ/kg for the cobalt oxide powder and 515 kJ/kg for the pellets were achieved.

More complex systems containing secondary oxide are being investigated to improve the properties or overcome the drawbacks of candidate materials for thermochemical heat storage. Generally, a secondary oxide addition to cobalt oxide was employed to increase anion vacancies concentration and increase oxygen mass transfer. Also, differences in oxidation state and atomic size cause a charge imbalance and lattice strain. The increased lattice vacancies density leads to higher oxygen mass transfer through the lattice. In addition to doping compounds, research continues in mixed metal oxides [38] and perovskites [39]. Basically, the cyclability of heat storage materials is improved by inhibiting grain growth using secondary oxide additions [1].

The effect of iron oxide addition to cobalt oxide was investigated by Block *et al.* [40]. They observed that the addition of iron oxide to cobalt oxide or the addition of cobalt oxide to iron oxide reduces the enthalpies of reaction in comparison with pure oxides. They reported that 10 mol% iron oxide doped cobalt oxide shows a high enthalpy of reaction and higher reduction/oxidation reversibility than pure cobalt oxide. The reversibility of the redox reactions of cobalt oxide pellets with the addition of alumina, ceria, iron oxide, manganese oxide, silicon carbide or zirconia in air flow and in the range of 800-1000 °C was also investigated by Pagkoura *et al.* [41]. They found that redox kinetics of cobalt oxide was improved with the addition of 25 wt% ceria, but the thermomechanical stability of the structured material did not improve. Also, they reported that cobalt oxide doped with 10-20 wt% of alumina or iron oxide showed good thermomechanical stability for 10 redox cycles while maintaining the thermochemical heat storage properties of cobalt oxide.

The main problem of cobalt oxide as a thermochemical heat storage material is low cyclability of redox reactions due to increasing grain size upon sintering during redox reactions. A large grain size reduces oxygen mass transfer and decreases the reaction kinetics specially the re-oxidation kinetics. Therefore, kinetics improvements are needed in order to make cobalt oxide usable as a thermochemical heat storage material. The re-oxidation kinetics of cobalt oxide is improved through the incorporation of secondary oxides [14].

Mechanical activation increases the reaction rates by making new features in the substance including structural disordering, structure relaxation, structural mobility, and an increase of specific surface area. These factors simultaneously affect the reactivity of a solid. Recently, mechanical activation has been used for improving the hydrogen desorption/absorption kinetics of hydrogen storage materials [42-45].

To the best knowledge of the authors, there is no report in the literature about effects of Fe₂O₃ addition and mechanical activation on the heat storage properties of cobalt oxide. Therefore, it seems that this research is a first attempt to evaluate the effect of mechanical activation along with Fe₂O₃ addition on the heat storage properties of cobalt oxide, which will provide useful background information on heat storage properties of cobalt oxide. The aim of the present work is to

investigate the mechanical activation effect along with Fe₂O₃ addition on the heat storage properties of cobalt oxide such as oxygen release and uptake, particle morphology, and redox cyclability under air atmosphere.

2. Experimental methods

2.1. Materials and preparation

Cobalt oxide and iron oxide specifications used in this research are shown in Table 1. Cobalt oxide was mixed with 2, 6, 10, 15, and 20 wt% of Fe₂O₃ and ball milled for 1 h using a high energy planetary ball mill (Retsch PM 100) equipped with a stainless steel vial (150 ml) and steel balls (diameter of 10 and 20 mm). Ball milling was carried out using a ball to powder weight ratio of 20 and a rotation speed of 300 rpm under air atmosphere.

2.2. Thermal analysis

Thermal analysis experiments (TG/DSC) were carried out by TA Instruments (SDT-Q600) analyzer using a sample weight of 15 mg, a heating rate of 5 °C/min, and an alumina crucible under an argon flow rate of 100 mL/min. In addition, a home designed thermogravimetry setup was used for studying the reduction and re-oxidation of samples under air atmosphere [46]. A cubic acrylic glass was used to avoid the effects of environmental airflow on the weight measuring system isolated in the setup. In each experiment, 5 g of the sample was poured in an alumina crucible (5×10×100 mm) and placed inside a quartz tube located in a tube furnace (Azar furnace 1250). Subsequently, a temperature range of 750 to 1050 °C with a heating/cooling rate of 5 °C/min was used for the reduction and re-oxidation processes. The weight change was recorded in real time using a digital balance (A&D model EK-600i) and software (RS weight A&D) linked and installed on a laptop.

Table 1. Raw materials specifications.

Material	Purity (wt%)	Particle size (µm)	Company
Cobalt oxide (Co ₃ O ₄)	99.5	10 <	B.D.H
Iron oxide (Fe ₂ O ₃)	99.5	10 <	Blulux

2.3. Materials characterization

The X-ray diffractometry (Italstructures APD2000) with $\text{CuK}\alpha$ radiation ($\lambda = 1.54 \text{ \AA}$) and X'Pert high score software (1.0d) were used for phase identification. Scanning electron microscopy (Jeol JSM-840A) was used for studying the powder morphology. Energy-dispersive X-ray spectroscopy (EDS) was used for x-ray map analysis.

3. Results and discussion

3.1. Effect of Fe_2O_3 addition and mechanical activation on Co_3O_4 redox reactions

The effect of iron oxide (2, 6, 10, 15, and 20 wt%) addition and 1 h mechanical activation on the redox reactions of Co_3O_4 was investigated by thermogravimetric analysis. The resulting TG curves of as-received Co_3O_4 , $\text{Co}_3\text{O}_4/1\text{h BM}$ and $\text{Co}_3\text{O}_4\text{-}15\text{wt}\% \text{Fe}_2\text{O}_3/1 \text{ h BM}$ samples are shown in Figure 1. The useful information including onset temperature of redox reactions and weight change are extracted from the TG curves and presented in Table 2. In Figure 1, the sample $\text{Co}_3\text{O}_4/1 \text{ h BM}$ shows weight increase in the early stage of the experiment. This phenomenon is due to CoO formation during ball milling and its re-oxidation in the early stage of the experiment. More details are provided in the previous work [46] of the authors.

According to Table 2, the reduction onset temperature of as-received Co_3O_4 and 1 h ball milled Co_3O_4 are 1030 and 1010 °C, respectively. Addition of 2 and 6 wt% of Fe_2O_3 to Co_3O_4 increases the reduction onset temperature to 1035 and 1050 °C, but addition of 10 and 15 wt% of Fe_2O_3 decreases the reduction onset temperature to 990 and 960 °C, respectively. More Fe_2O_3 addition (20 wt%) increases the reduction onset temperature to about

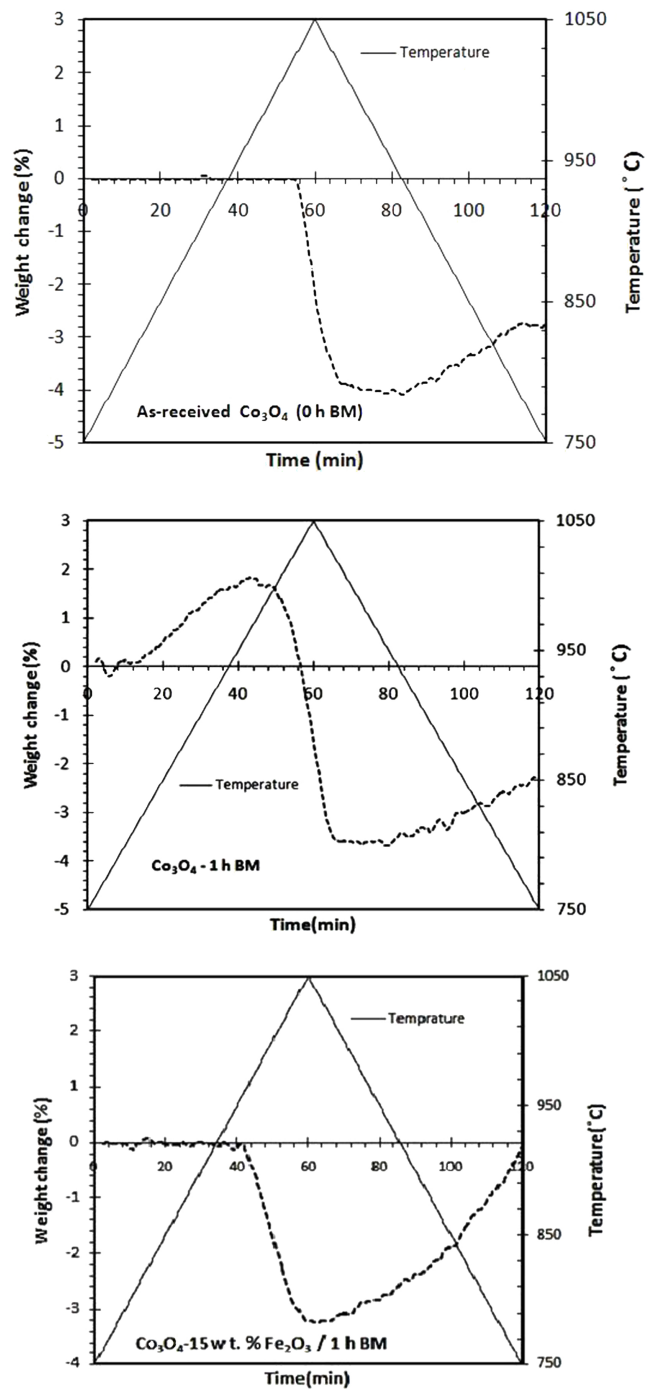


Fig. 1. TG curve of as-received Co_3O_4 , $\text{Co}_3\text{O}_4/1\text{h BM}$ and $\text{Co}_3\text{O}_4\text{-}15\text{wt}\% \text{Fe}_2\text{O}_3 / 1 \text{ h BM}$ samples.

Table 2. Thermodynamic data obtained by thermogravimetry under air atmosphere.

Sample	Onset- T_{red} (°C)	Onset- T_{oxid} (°C)	Δm_{red} (%)	$\Delta m_{\text{re-oxid}}$ (%)
As-received Co_3O_4	1030	930	4.0	1.4
Co_3O_4 -1 h BM	1010	950	3.5	1.2
Co_3O_4 - 2 wt% Fe_2O_3	1035	930	1.4	1.5
Co_3O_4 - 6 wt% Fe_2O_3	1050	980	1.7	1.8
Co_3O_4 - 10 wt% Fe_2O_3	990	980	3.2	3.5
Co_3O_4 - 15 wt% Fe_2O_3	960	1010	3.4	3.3
Co_3O_4 - 20 wt% Fe_2O_3	1030	1010	0.9	1.0

1030 °C again. Generally, it is clear that increasing the Fe_2O_3 content in the samples increases the oxidation onset temperature.

Another important result is a difference between onset temperature of reduction and re-oxidation. The closer reduction and re-oxidation onset temperature, the lower energy loss during charge and discharge. This is a very favorable effect in view of thermal energy storage. The difference between reduction and re-oxidation onset temperatures for as-received cobalt oxide is about 100 °C. It decreases as the Fe_2O_3 content of the samples increases.

Also, Table 2 shows that Fe_2O_3 addition from 2 to 15 wt% increases the oxygen release (Δm_{red}) from 1.4 to 3.4 wt%. This means that Fe_2O_3 addition up to 15 wt% improves the oxygen release. However, increasing the Fe_2O_3 content to 20 wt% decreases the oxygen release to 0.9 wt%. In contrary, the oxygen release of as-received Co_3O_4 and 1 h BM Co_3O_4 are 4 and 3.5 wt%, respectively. It must be said that total theoretical weight change is 6.64 wt% during reduction and re-oxidation stages. Therefore, it is observed that all of the samples weight change is less than the theoretical value.

The oxygen uptake value increases from 1.5 to 3.3 wt% for samples containing 2 and 15 wt% Fe_2O_3 , respectively. Addition of 20 wt% Fe_2O_3 decreased the oxygen uptake to 1 wt%. As previously stated, the main problem of Co_3O_4 as a heat storage material is its weak re-oxidation behavior. According to Table 2, although Fe_2O_3 addition decreases the oxygen release value in comparison with as-received cobalt oxide and 1 h ball milled cobalt oxide, Fe_2O_3 addition (up to 15 wt%) considerably improves the oxygen uptake value or re-oxidation behavior.

Another important point according to Table 2 is that oxygen release and uptake values for samples containing Fe_2O_3 are close, but their values are different for as-received Co_3O_4 and 1 h ball milled Co_3O_4 . The reason for the similarity between oxygen release and uptake values for Fe_2O_3 containing samples are low sintering of particles. This phenomenon has been reported by various researchers [14,30,34].

The different behavior of samples containing 20 wt% Fe_2O_3 is most probably due to the formation of Co_3O_4 and Fe_3O_4 spinels (according to Figure 2) that release or uptake oxygen at high temperatures [40]. The formation range of the spinel phase in the Co_3O_4 - Fe_2O_3 phase diagram has been investigated in various research works

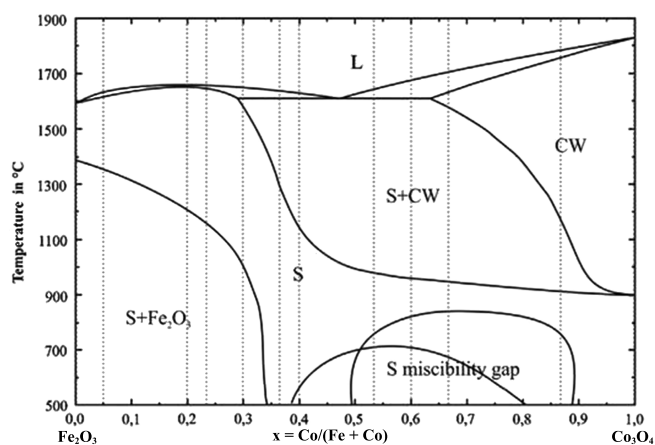


Fig. 2. Phase diagram of the Co–Fe–O system with material compositions (dotted lines) (S: spinel, CW: cobalt-wüstite, L: liquid) [40].

[30,33], but it must be noted that mechanical activation may change the phase stability regions [44,45].

3.2. Morphology of particles

Figure 3 illustrates the particle morphologies of as-received Co_3O_4 , 1 h ball milled Co_3O_4 , and 1 h ball milled Co_3O_4 -15 wt% Fe_2O_3 samples before and after redox. It is seen that the Fe_2O_3 containing sample was less sintered than the other two samples. Therefore, Fe_2O_3 addition plays a key role in decreasing the particle sintering and growth. According to Figure 3, the particle size of as-received Co_3O_4 and 1 h ball milled Co_3O_4 after redox are several times larger than before redox, while the particle size of 1 h ball milled Co_3O_4 -15 wt% Fe_2O_3 show low growth after redox. In fact, Fe_2O_3 particles are placed among the Co_3O_4 particles and prevent the cobalt oxide particle adhesion and sintering due to a higher melting point than cobalt oxide. Figure 4 shows the x-ray map analysis for the Co_3O_4 -15 wt% Fe_2O_3 /1 h BM sample after redox. Figure 4 demonstrates that the iron oxide particles have dispersed uniformly in the sample and around the cobalt oxide particles.

3.3. TG/DSC analysis under argon atmosphere

For studying the synergistic effect of Fe_2O_3 addition and mechanical activation on the oxygen release and heat storage value under an oxygen partial pressure close to zero, three samples including as-received Co_3O_4 , 1 h ball milled Co_3O_4 , and 1 h ball milled Co_3O_4 -15% Fe_2O_3 were analyzed by TG/DSC under argon

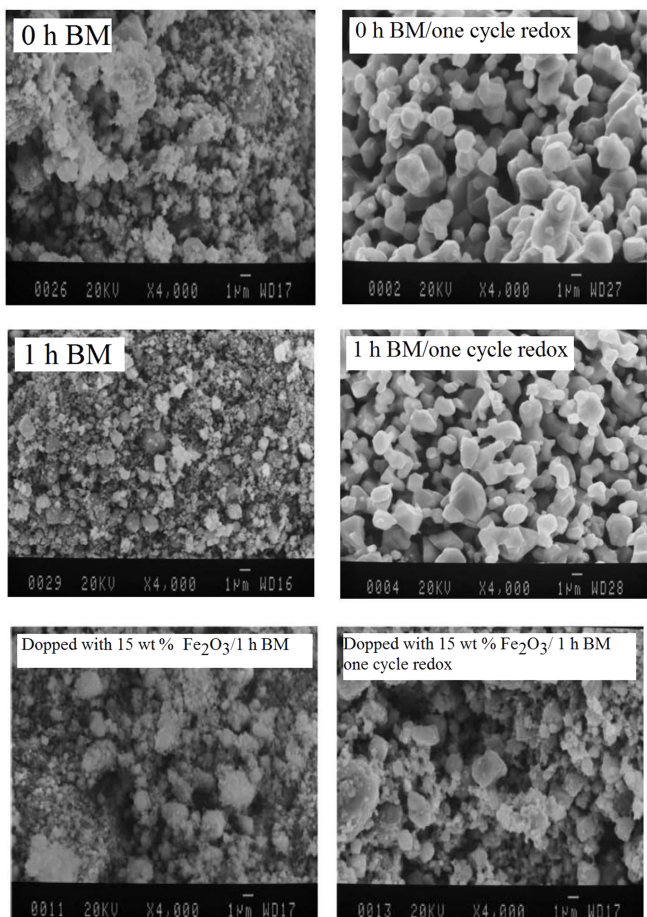


Fig. 3. SEM images of as-received Co_3O_4 , $\text{Co}_3\text{O}_4/1\text{h BM}$ and $\text{Co}_3\text{O}_4-15\text{ wt}\% \text{Fe}_2\text{O}_3/1\text{h BM}$ before and after redox.

atmosphere and heating rate of $5\text{ }^\circ\text{C}/\text{min}$. It should be noted that the oxidation reaction was not done, because the re-oxidation reaction takes place only in oxygen

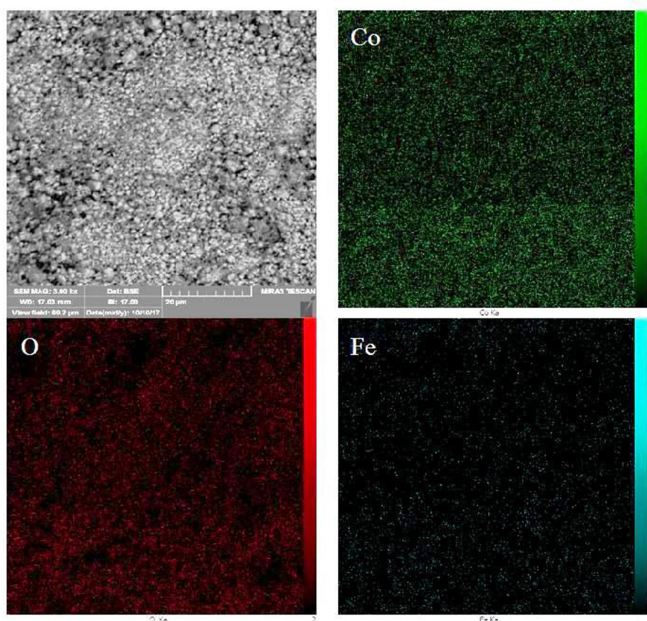


Fig. 4. X-ray map analyses of $\text{Co}_3\text{O}_4-15\text{ wt}\% \text{Fe}_2\text{O}_3$ sample after redox.

containing environment. It was not possible to decide on the synergistic effect of Fe_2O_3 addition and mechanical activation according to the experiments carried out under air atmosphere, because the oxygen partial pressure is different in the reaction medium of various samples due to their different oxygen release.

According to Figure 5, total weight loss of the above mentioned samples are 6.5, 6.3, and 5.8 wt%, respectively. These values are different from the weight decrease presented in Table 2. This is due to the fact that argon gas dilutes the oxygen in the reaction medium while it facilitates the reaction of cobalt oxide reduction. In addition, the sample weight (15 mg versus 5 g) has an effective on the weight loss/increase value. At high sample weights, the heat transfer from outside/inside into the sample in the reduction/re-oxidation stage is important because it takes a long time. Moreover, the partial pressure of the oxygen around the samples tested under the air atmosphere is different, while it is alike in the experiments carried out under the argon atmosphere. Due to the above-mentioned reasons, the onset temperature of reduction is almost the same for the samples tested under the argon atmosphere and are different for the samples tested under the air atmosphere.

The theoretical weight loss of the Co_3O_4 is close to 6.64 wt%. If it is considered that only the Co_3O_4 fraction of $\text{Co}_3\text{O}_4-15\text{ wt}\% \text{Fe}_2\text{O}_3$ participates in the reduction process, the theoretical loss weight of the sample will be 5.64 wt%. However, the practical obtained oxygen release value of the mentioned sample was 5.8 wt% (0.16 wt% more than the theoretical value). This only

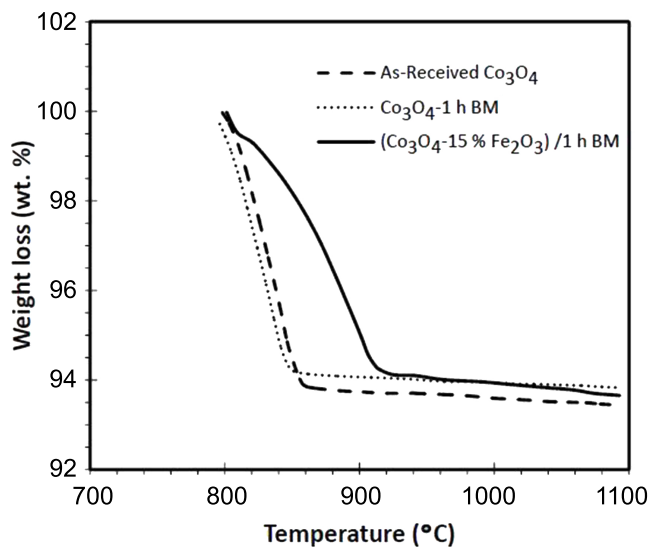


Fig. 5. TG curves of as-received Co_3O_4 , 1 h ball milled Co_3O_4 , and $\text{Co}_3\text{O}_4-15\text{ wt}\% \text{Fe}_2\text{O}_3/1\text{ h BM}$.

happens when some of the Fe_2O_3 is reduced to Fe_3O_4 . Therefore, it seems that in addition to cobalt oxide, Fe_2O_3 also participates in the reduction process. According to the difference (0.16 wt%) between theoretical and practical oxygen release, the amount of formed Fe_3O_4 will be about 5 wt%; and therefore, its XRD peaks have low intensity. According to Figure 6, only Fe_2O_3 phase peaks are seen in the XRD pattern related to before reduction; but after reduction both Fe_2O_3 and Fe_3O_4 peaks exist in the XRD pattern. It should be noted that the presence of Fe_3O_4 after reduction is based on the XRD patterns and TG results.

According to DSC results (Figure 7), the absorbed heat energy for reduction of as-received Co_3O_4 , 1 h mechanical activated Co_3O_4 , and 1 h ball milled Co_3O_4 -15% Fe_2O_3 are 622, 496, and 895 kJ/kg, respectively. These values were taken directly from the device (SDT-Q600) and are proportional to the area under the endothermic peaks in Figure 7. As it is seen, 1 h ball milled Co_3O_4 , in comparison with other two samples, has absorbed low heat energy because some part of the energy required for reduction is compensated by the energy stored in the Co_3O_4 structure during ball milling. It can also be seen that the 1 h ball milled Co_3O_4 -15% Fe_2O_3 has absorbed higher heat energy, even higher than the theoretical value (717.4 kJ/kg), due to the reduction of Fe_2O_3 to Fe_3O_4 . The temperature of Fe_2O_3 reduction to Fe_3O_4 is about 100 °C higher than that of Co_3O_4 reduction to CoO [14]. The XRD patterns of Co_3O_4 -15% Fe_2O_3 sample before and after redox shown in Figure 6 confirmed the presence of Fe_3O_4 after the reduction. In fact, the high energy ball milling decreases the temperature of Fe_2O_3 reduction to Fe_3O_4 [44,45].

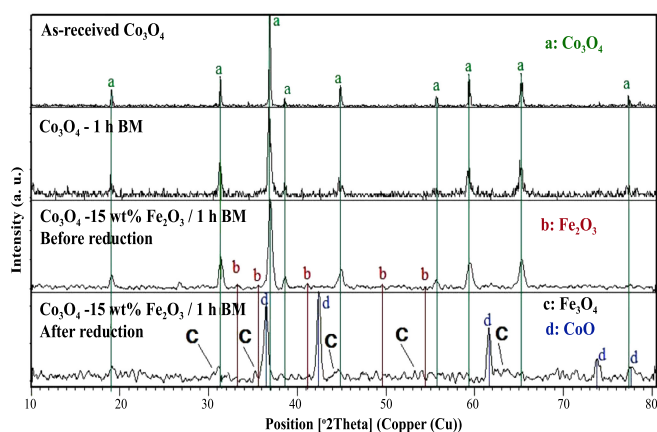


Fig. 6. XRD patterns of as-received Co_3O_4 , 1 h ball milled Co_3O_4 , and Co_3O_4 -15 wt% Fe_2O_3 /1 h BM before and after reduction.

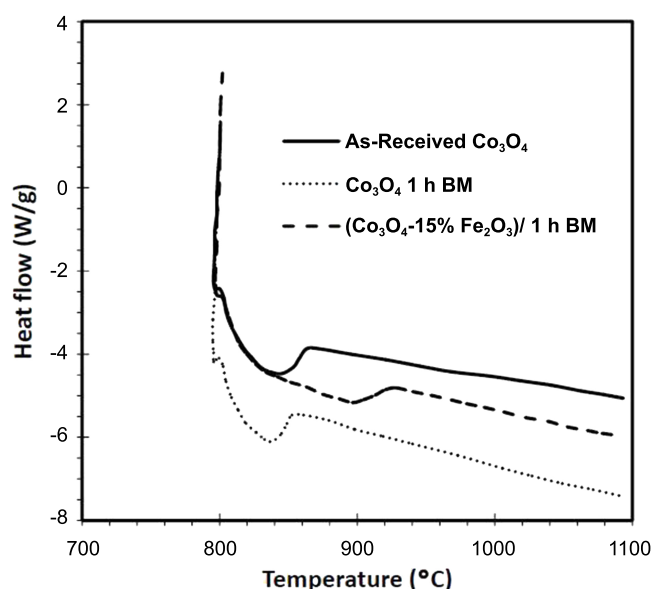


Fig. 7. DSC curves of as-received Co_3O_4 , 1 h ball milled Co_3O_4 , and Co_3O_4 -15 wt% Fe_2O_3 /1 h BM.

Moreover, according to Figure 7, Fe_2O_3 addition has caused the heat energy absorption to take place in a wide range of temperature or time in comparison with the other two samples. This means that heat charge and discharge processes in samples containing iron oxide are more controllable.

3.4. Redox cyclability

The redox cyclability of the as-received Co_3O_4 and 1 h ball milled Co_3O_4 -15% Fe_2O_3 samples under air atmosphere and a heating/cooling rate of 5 °C/min for 3 cycles were investigated. Figure 8 illustrates the cyclability results. It is seen that weight loss and weight increase of as-received Co_3O_4 decreased gradually as the cycle numbers increased and reached from 3 wt% at cycle one to about 1.5 wt% at cycle three. The cyclability of the 1 h ball milled sample disappears after two cycles. More details about the cyclability of this sample are found in the previous work of the authors [46]. However, the cyclability of Co_3O_4 -15 wt% Fe_2O_3 is favorable in comparison with as-received and 1 h ball milled samples. The reason the cyclability improves with the addition of iron oxide is due to low particles growth and sintering.

4. Conclusions

This research obtained the following results:

- Fe_2O_3 addition from 2 to 15 wt% increased the

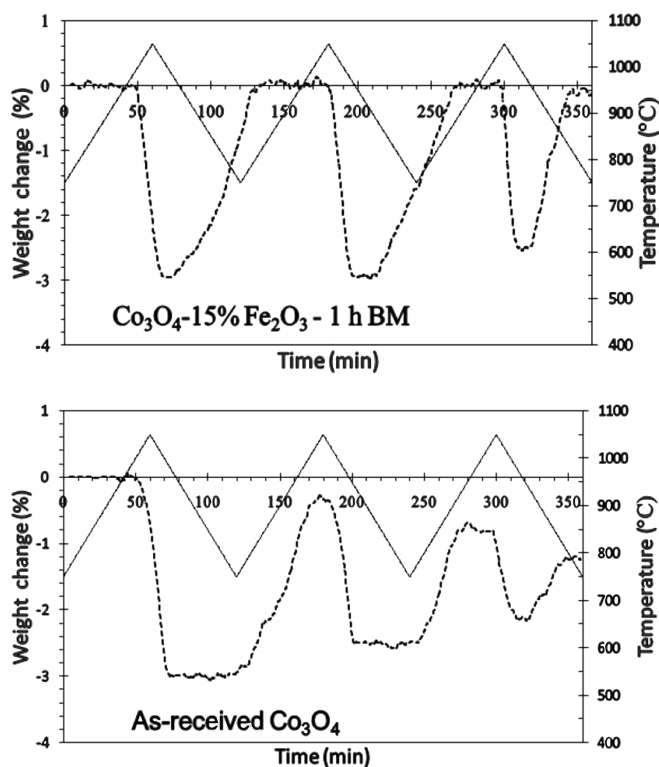


Fig. 8. Cyclability of as-received Co_3O_4 and 1 h ball milled Co_3O_4 -15 wt% Fe_2O_3 .

oxygen release from 1.4 to 3.4 wt% and decreased the reduction onset temperature from 1030 to 960 °C.

- Oxygen uptake value and re-oxidation onset temperature increased from 1.5 to 3.3 wt% and from 930 to 1010 °C for the samples containing 2 and 15 wt% Fe_2O_3 , respectively.

- TG/DSC analysis under argon atmosphere revealed that enthalpy of reduction reaction of as-received Co_3O_4 , 1 h ball milled Co_3O_4 and 1 h ball milled Co_3O_4 -15 wt% Fe_2O_3 is 622, 496, and 895 kJ/kg, respectively.

- Phase identification by XRD and related TG analysis demonstrated that Fe_2O_3 participates in the reduction process.

- Fe_2O_3 addition prevented the cobalt oxide particle growth and sintering; subsequently, it improved the re-oxidation behavior.

- Addition of 15 wt% Fe_2O_3 to Co_3O_4 and ball milling of the mixture for 1 h improved the redox cyclability.

Acknowledgment

The authors wish to thank Mr. A. Nsari for his assistance during the experiments. This work was supported by Hamadan University of Technology [Grant No. 18-94-1-361].

References

- [1] L. Andre, S. Abanades, G. Flamant, Screening of thermochemical systems based on solid-gas reversible reactions for high temperature solar thermal energy storage, *Renew. Sušt. Energ. Rev.* 64 (2016) 703-715.
- [2] A.J. Carrillo, J. Moya, A. Bayon, P. Jana, V.A. de la Pena OShea, M. Romero, J. Gonzalez-Aguilar, D.P. Serrano, P. Pizarro, J.M. Coronado, Thermochemical energy storage at high temperature via redox cycles of Mn and Co oxides: Pure oxides versus mixed ones, *Sol. Energy. Mat. Sol. C.* 123 (2014) 47-57.
- [3] N.P. Siegel, Thermal energy storage for solar power production, *Wires Energy Environ.* 1 (2012) 119-131.
- [4] S. Kuravi, J. Trahan, Y. Goswami, M.M. Rahman, E.K. Stefanakos, Thermal energy storage technologies and systems for concentrating solar power plants, *Prog. Energy Combust.* 39 (2013) 285-319.
- [5] T. M. I. Mahlia, T.J. Saktisahdan, A. Jannifar, M.H. Hasan, H.S.C. Matseelar, A review of available methods and development on energy storage; technology update, *Renew. Sušt. Energ. Rev.* 33 (2014) 532-454.
- [6] P. Pardo, A. Deydier, Z. Anxionnaz-Minvielle, S. Rougé, M. Cabassud, P. Cognet, A review on high temperature thermochemical heat energy storage, *Renew. Sušt. Energ. Rev.* 32 (2014) 591-610.
- [7] T. Yan, R.Z. Wang, T.X. Li, L.W. Wang, I.T. Fred, A review of promising candidate reactions for chemical heat storage, *Renew. Sušt. Energ. Rev.* 43 (2015) 13-31.
- [8] C. Agrafiotis, A. Becker, M. Roeb, C. Sattler, D. Zentrum, Exploitation of thermochemical cycles based on solid oxide redox systems for thermochemical storage of solar heat. Part 5: Testing of porous ceramic honeycomb and foam cascades based on cobalt and manganese oxides for hybrid sensible/thermochemical heat storage, *Sol. Energy*, 139 (2016) 676-694.
- [9] M. Romero, A. Steinfeld, Concentrating solar thermal power and thermochemical fuels, *Energ. Environ. Sci.* 5 (2012) 9234-9245.
- [10] L. Cabeza, *Advances in Thermal Energy Storage System*, Cambridge, UK, 2015.
- [11] C. Agrafiotis, M. Roeb, M. Schmucker, C. Sattler, Exploitation of thermochemical cycles based on solid

- oxide redox systems for thermochemical storage of solar heat. Part 1: Testing of cobalt oxide-based powders, *Sol. Energy*, 102 (2014) 189-211.
- [12] J.E. Funk, R.M. Reinstrom, Energy requirements in production of hydrogen from water, *Ind. Eng. Chem. Procs. D. D.* 5 (1966) 336-342.
- [13] F. Schaube, A. Wörner, and R. Tamme, High temperature thermochemical, heat storage for concentrated solar power using gas-solid reactions, *J. Sol. Energ. -T ASME*, 133 (2011) 031006.
- [14] B. Wong, Thermochemical heat storage for concentrated solar power. In: Final Report for the U.S. Department of Energy 2011, General Atomics, 3550 General Atomics Court, San Diego CA92037: San Diego, CA, USA.
- [15] R. Chacartegui, A. Alovio, C. Ortiz, J.M. Valverde, V. Verda, J.A. Becerra, Thermochemical energy storage of concentrated solar power by integration of the calcium looping process and a CO₂ power cycle, *Appl. Energ.* 173 (2016) 589-605.
- [16] F. Schaube, L. Koch, A. Wörner, H. Müller-Steinhagen, A thermodynamic and kinetic study of the de- and rehydration of Ca(OH)₂ at high H₂O partial pressures for thermo-chemical heat storage, *Thermochim. Acta*, 538 (2012) 9-20.
- [17] M. Schmidt, C. Szczukowski, C. Roßkopf, M. Linder, A. Wörner, Experimental results of a 10 kW high temperature thermochemical storage reactor based on calcium hydroxide, *Appl. Therm. Eng.* 62 (2014) 553-559.
- [18] J. Yan, C.Y. Zhao, Experimental study of CaO/Ca(OH)₂ in a fixed-bed reactor for thermochemical heat storage, *Appl. Energ.* 175 (2016) 277-284.
- [19] M. Tmar, C. Bernard, M. Ducarroir, Local storage of solar energy by reversible reactions with sulfates, *Sol. Energy*, 26 (1981) 529-536.
- [20] K. Lovegrove, A. Luzzi, I. Soldiani, H. Kreetz, Developing ammonia based thermochemical energy storage for dish power plants, *Sol. Energy*, 76 (2004) 331-337.
- [21] M. Rydén, H. Leion, T. Mattisson, A. Lyngfelt, Combined oxides as oxygen-carrier material for chemical-looping with oxygen uncoupling, *Appl. Energ.* 113 (2014) 1924-1932.
- [22] K.N. Hutchings, M. Wilson, P.A. Larsen, R.A. Cutler, Kinetic and thermodynamic considerations for oxygen absorption/desorption using cobalt oxide, *Solid State Ionics*, 177 (2006) 177 45-51.
- [23] C. Agrafiotis, M. Roeb, M. Schmücker, C. Sattler, Exploitation of thermochemical cycles based on solid oxide redox systems for thermochemical storage of solar heat. Part 2: redox oxide-coated porous ceramic structures as integrated thermochemical reactors/heat exchangers, *Sol. Energy*, 114 (2015) 440-458.
- [24] M. Neises, S. Tescari, L. de Oliveira, M. Roeb, C. Sattler, B. Wong, Solar-heated rotary kiln for thermochemical energy storage, *Sol. Energy*, 86 (2012) 3040-3048.
- [25] A.P. Muroyama, A.J. Schrader, P.G. Loutzenhiser, Solar electricity via an Air Brayton cycle with an integrated two-step thermochemical cycle for heat storage based on Co₃O₄/CoO redox reactions II: kinetic analyses, *Sol. Energy*, 122 (2015) 409-418.
- [26] A.J. Carrillo, D. Saestre, D.P. Serrano, P. Pizarroab, J.M. Coronado, Revisiting the BaO₂/BaO redox cycle for solar thermochemical energy storage, *Phys. Chem. Chem. Phys.* 18 (2016) 8039-8048.
- [27] A.J. Carrillo, D.P. Serrano, P. Pizarro, J.M. Coronado, Thermochemical heat storage based on the Mn₂O₃/Mn₃O₄ redox couple: influence of the initial particle size on the morphological evolution and cyclability, *J. Mater. Chem. A*, 2 (2014) 19435-19443.
- [28] M. Wokon, A. Kohzer, A. Benzarti, T. Bauer, M. Linder, A. Wörner, Thermochemical energy storage based on the reversible reaction of metal oxides, In: 3rd International conference on chemical looping, Göteborg, Sweden, September 9-11, 2014.
- [29] E. Alonso, C. Pérez-Rábago, J. Licurgo, E. Fuentealba, C.A. Estrada, First experimental studies of solar redox reactions of copper oxides for thermochemical energy storage, *Sol. Energy*, 115 (2015) 297-305.
- [30] T. Block, M. Schmücker, Metal oxides for thermochemical energy storage: a comparison of several metal oxide systems, *Sol. Energy*, 126 (2016) 195-207.
- [31] S.M. Babiniec, E.N. Coker, J.E. Miller, A. Ambrosini, Investigation of La_xSr_{1-x}Co_yM_{1-y}O_{3-δ} (M= Mn, Fe) perovskite materials as thermochemical energy storage media, *Sol. Energy*, 118 (2015) 451-459.
- [32] S.M. Babiniec, E.N. Coker, J.E. Miller, A. Ambrosini, Doped calcium manganites for advanced high-temperature thermochemical energy storage, *Int. J. Energ. Res.* 40 (2016) 280-284.

- [33] K.J. Albrecht, G.S. Jackson, R.J. Braun, Thermodynamically consistent modeling of redox-stable perovskite oxides for thermochemical energy conversion and storage, *Appl. Energ.* 165 (2016) 285-96.
- [34] B. Wong, L. Brown, F. Schaube, R. Tamme, C. Sattler, Oxide based thermochemical heat storage, In: Presented at Solar PACES, Perpignan, France, 2010.
- [35] C. Agrafiotis, S. Tescari, M. Roeb, M. Schmucker, C. Sattler, Exploitation of thermochemical cycles based on solid oxide redox systems for thermochemical storage of solar heat. Part 3: Cobalt oxide monolithic porous structures as integrated thermochemical reactors/heat exchangers, *Sol. Energy*, 114 (2015) 459-475.
- [36] S. Tescari, C. Agrafiotis, S. Breuer, L. De Oliveira, M. Nieves-von Puttkamer, M. Roeb, C. Sattler, Thermochemical solar energy storage via redox oxides: materials and reactor/heat exchanger concepts, *Energ. Proced.* 49 (2014) 1034-1043.
- [37] G. Karagiannakis, C. Pagkoura, A. Zygogianni, S. Lorentzou, A.G. Konstandopoulos, Monolithic ceramic redox materials for thermochemical heat storage applications in CSP plants, *Energ. Proced.* 49 (2014) 820-829.
- [38] B. Ehrhart, E. Coker, N. Siegel, A. Weimer, Thermochemical cycle of a mixed oxide for augmentation of thermal energy storage in solid particles, *Energ. Proced.* 49 (2014) 762-771.
- [39] Y.S. Lin, Q. Yang, J. Ida, High temperature sorption of carbon dioxide on perovskite-type metal oxides, *J. Taiwan Inst. Chem. E.* 40 (2009) 276-780.
- [40] T. Block, N. Knoblauch, M. Shmücker, The cobalt-oxide/iron-oxide binary system for use as high temperature thermochemical energy storage material, *Thermochim. Acta*, 577 (2014) 25-32.
- [41] C. Pagkoura, G. Karagiannakis, A. Zygogianni, S. Lorentzou, M. Kostoglou, A.G. Konstandopoulos, M. Rattenbury, W.J. Woodhead, Cobalt oxide based structured bodies as redox thermochemical heat storage medium for future CSP plants, *Sol. Energy*, 108 (2014) 146-163.
- [42] V. Varin, T. Czujko, S. Wronski, *Nanomaterials for Solid State Hydrogen Storage*, Springer, USA, 2009.
- [43] P.R. Soni, *Mechanical Alloying: Fundamentals and Applications*, first ed., Cambridge International Science Publishing, UK, 2001.
- [44] P. Balaz, *Extractive Metallurgy of Activated Minerals*, Elsevier, Amsterdam, 2000.
- [45] C. Suryanarayana, *Mechanical Alloying and Milling*, first ed., Marcel Dekker, New York, 2004.
- [46] N. Nekokar, M. Pourabdoli, A. Ghaderi Hamidi, D. Uner, Effect of mechanical activation on thermal energy storage of $\text{Co}_3\text{O}_4/\text{CoO}$ system, *Adv. Powder Technol.* 29 (2018) 333-340.